

Experimental observations of flow and bed morphology in a meandering compound channel with variable density floodplain vegetation

Daniel C. White, PhD Candidate, Colorado State University, Fort Collins, CO,
danny.white@colostate.edu

Ryan R. Morrison, Associate Professor, Colorado State University, Fort Collins, CO,
ryan.morrison@colostate.edu

Peter A. Nelson, Associate Professor, Colorado State University, Fort Collins, CO,
peter.nelson@colostate.edu

Introduction

Floodplain vegetation has been recognized for providing important ecosystem services to both humans and the aquatic and terrestrial organisms that inhabit riparian corridors. These ecological functions and ecosystem services often depend on floods, which produce hydrologic exchange flows – the transfer of water between a river channel and floodplain surface. Predicting the hydraulic nature of floods is difficult because of the complex flow patterns that develop over vegetated floodplains, at the channel-floodplain boundary, and within the active channel. In river restoration design and management applications, simulating oversimplified hydraulic conditions of floods may result in poor design and projects that ultimately fail to meet defined goals as channels respond to the stresses of a flood.

To gain insight into how floodplain vegetation impacts flow and channel morphology during floods in meandering compound channels, we conducted a series of mobile-bed flume experiments in which discharge, flow depth, and floodplain vegetation density were varied. Distinct from meandering compound experiments performed and discussed in the literature (Shiono et al., 2009a, 2009b), we varied the density of rigid emergent vegetation elements on the floodplain and incrementally monitored bed evolution until quasi-equilibrium conditions were reached for each of seven scenarios.

Methodology

The flume centerline followed a sine-generated trace with a 30-degree crossing angle. The channel was 1-meter wide inset in a 15.4-meter long, 4.9-meter wide basin (See Figure 1). We tested bare and vegetated floodplain conditions with 2.67-centimeter diameter emergent, cylindrical elements at spacings of 3.0 stems/m² and 12.1 stems/m². Flow depths ranged from bankfull to a relative depth (D_r , the ratio of floodplain depth to bankfull depth) of 0.25 (See Table 1.). The bed was composed of mobile sand-and-gravel sediment with a D_{50} of 3.3 mm.

Water was pumped into the channel at a steady rate and sediment was fed into the channel at a rate that matched the transport as measured by dried sediment which had accumulated in the downstream tail box over the course of each run. This was continued for each scenario until the channel reached equilibrium between sediment input and output. We then measured bed morphology, 3D flow field, and sediment transport for each experiment. We used structure-from-motion photogrammetry following Morgan et al. (2017) to measure bed morphology at

sub-cm resolution referenced to a local coordinate system. We measured the flow field in the channel at ten cross-sections (See Figure 1.) using a Nortek Vectrino profiling acoustic doppler velocimeter and a Nortek Vectrino+ single point ADV. Surface velocities were measured using large scale particle image velocimetry (LSPIV) processed in Fudaa-LSPIV.

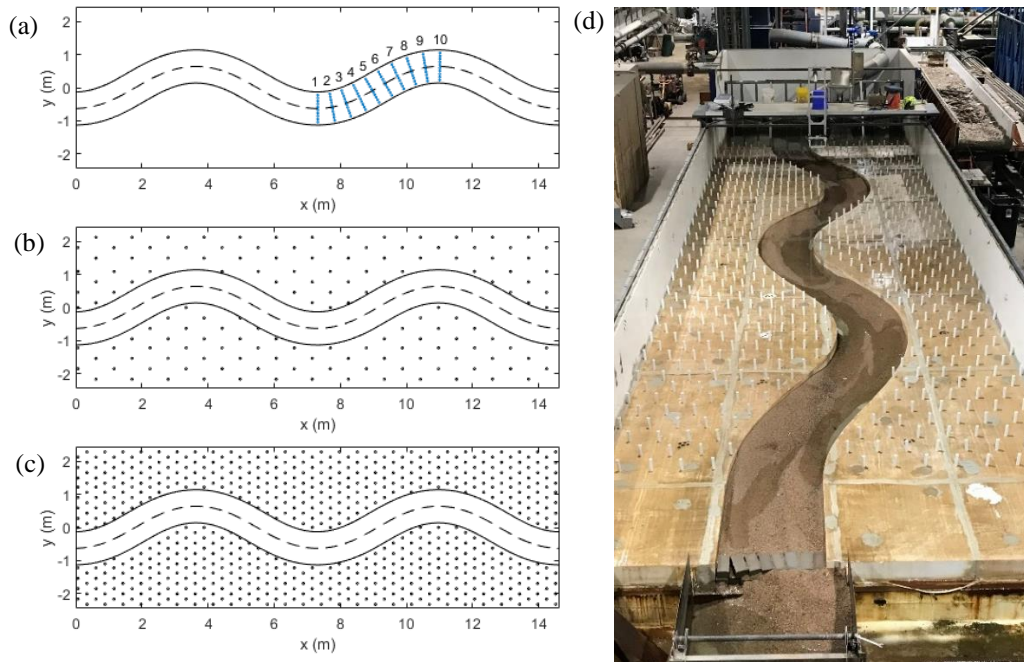


Figure 1. Flume configuration and floodplain cover scenarios. (a) No floodplain vegetation. Blue dots represent in-channel velocity measurement transects. (b) Low density floodplain vegetation. (c) High density floodplain vegetation. (d) Photo of flume with high density floodplain vegetation.

SfM point clouds were processed in Agisoft Metashape (“Agisoft Metashape Professional,” 2022) and converted to DEMs with a 0.005 m grid using Kriging interpolation for topographic differencing. Each DEM was detrended in the downvalley direction so that the elevation of each DEM grid cell was relative to the average gridded column elevation.

Table 1. Flume run scenario parameters

Run	Discharge	Sediment Supply	Floodplain Vegetation	Relative Depth
1	0.04 m ³ /s	5 kg/hr	NA	bankfull
2	0.08 m ³ /s	2.5 kg/hr	0	0.1
3	0.08 m ³ /s	2.5 kg/hr	Low - 3.0 cylinders/m ²	0.1
4	0.08 m ³ /s	2.5 kg/hr	High - 12.1 cylinders/m ²	0.1
5	0.18 m ³ /s	80 kg/hr	High - 12.1 cylinders/m ²	0.25
6	0.17 m ³ /s	65 kg/hr	Low - 3.0 cylinders/m ²	0.25
7	0.16 m ³ /s	60 kg/hr	0	0.25

Results

Flow Field

3D velocity measurements through the water column were taken at ten equally spaced stations across each cross-section. The velocity profiles measured at cross-section 10 are presented in Figure 2. Secondary current strength increased with floodplain vegetation density for both relative depth scenarios. Exchange flow from channel to floodplain decreased with vegetation density as energy is attenuated at the channel-floodplain interface.

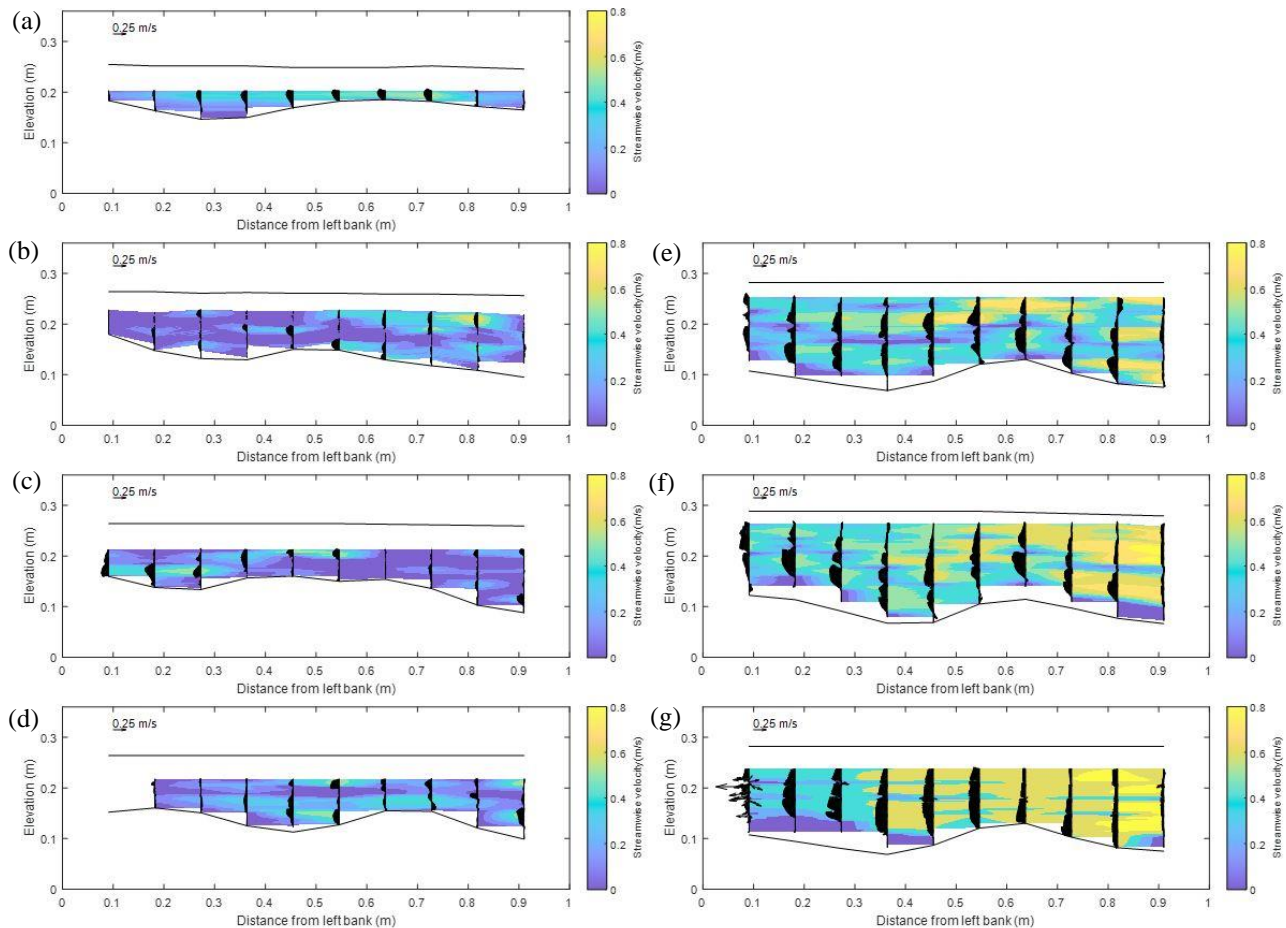


Figure 2. Cross-section velocity profiles for flume run scenarios. The contour map represents the streamwise velocity magnitude, and black lines represent lateral and vertical components of velocity measurements. (a) Bankfull, (b) $D_r = 0.1$, bare floodplain, (c) $D_r = 0.1$, low density vegetation, (d) $D_r = 0.1$, high density vegetation, (e) $D_r = 0.25$, bare floodplain, (f) $D_r = 0.25$, low density vegetation, (g) $D_r = 0.25$, high density vegetation

Bed morphology

Bed topography was recorded for each experimental scenario and is presented in Figure 3. At low relative depth, pool width increased with increased floodplain vegetation density, which may be attributed to an increase in the strength of secondary currents as floodplain vegetation

steers flows toward the channel. At high relative depth ($D_r = 0.25$), bedforms became more pronounced with greater bar-pool relief as floodplain vegetation density increased. The flow field within the active channel was altered due to the hydraulic interaction of overbank flows with floodplain vegetation.

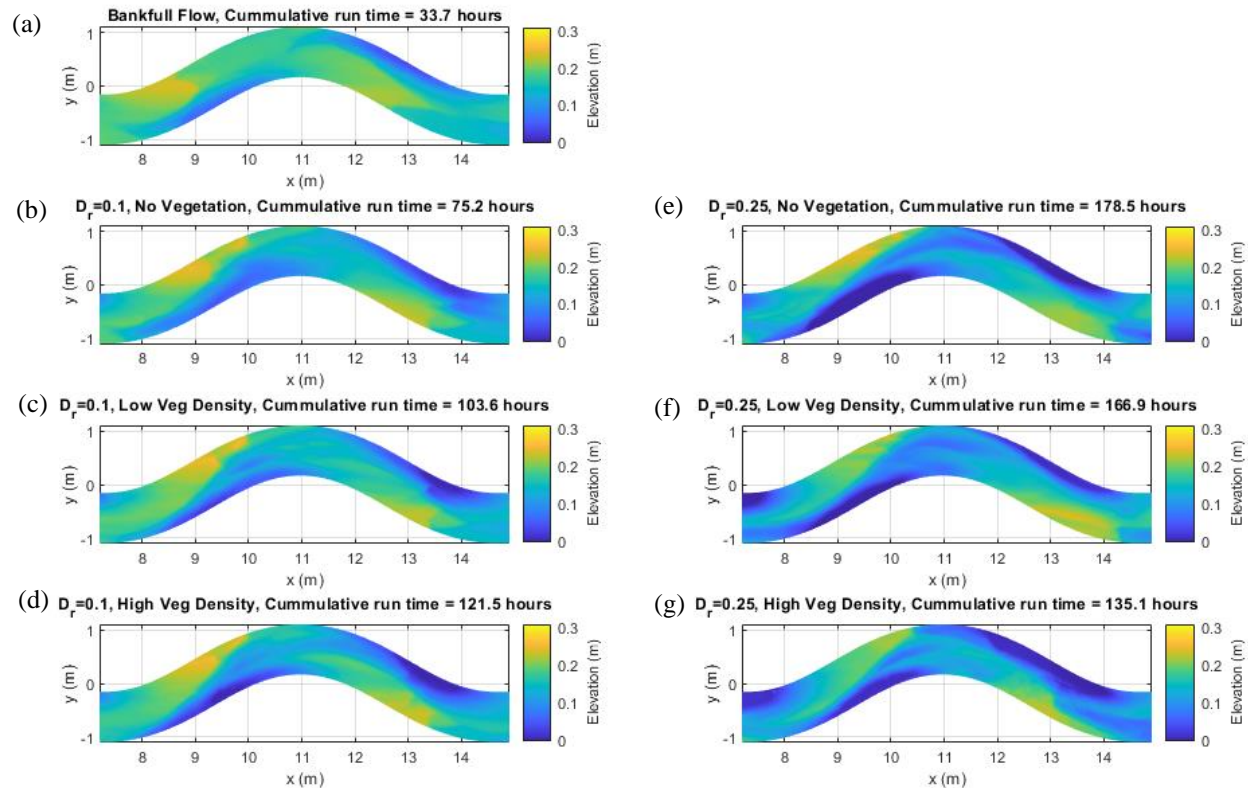


Figure 3. Quasi-equilibrium bed topography at downstream meander bend for each of the seven different flume run scenarios. (a) Bankfull, (b) $D_r = 0.1$, bare floodplain, (c) $D_r = 0.1$, low density vegetation, (d) $D_r = 0.1$, high density vegetation, (e) $D_r = 0.25$, bare floodplain, (f) $D_r = 0.25$, low density vegetation, (g) $D_r = 0.25$, high density vegetation.

References

- Agisoft Metashape Professional. (2022). (Version 1.8.1). Agisoft LLC. Retrieved from <http://www.agisoft.com>
- Morgan, J. A., Brogan, D. J., & Nelson, P. A. (2017). Application of Structure-from-Motion photogrammetry in laboratory flumes. *Geomorphology*, 276, 125–143. <https://doi.org/10.1016/j.geomorph.2016.10.021>
- Shiono, K., Chan, T. L., Spooner, J., Rameshwaran, P., & Chandler, J. H. (2009a). The effect of floodplain roughness on flow structures, bedforms and sediment transport rates in meandering channels with overbank flows: Part I. *Journal of Hydraulic Research*, 47(1), 5–19. <https://doi.org/10.3826/jhr.2009.2944-I>
- Shiono, K., Chan, T. L., Spooner, J., Rameshwaran, P., & Chandler, J. H. (2009b). The effect of floodplain roughness on flow structures, bedforms and sediment transport rates in meandering channels with overbank flows: Part II. *Journal of Hydraulic Research*, 47(1), 20–28. <https://doi.org/10.3826/jhr.2009.2944-II>